Deep Learning-based Trichoscopic Image Analysis and Quantitative Model for Predicting Basic and Specific Classification in Male Androgenetic Alopecia

Meng GAO[1], Yue WANG[2], Haipeng XU[3], Congcong XU[1], Xianhong YANG[1], Jin NIE[1], Ziye ZHANG[1], Zhixuan LI[2], Wei HOU[1] and Yiqun JIANG[1]

[1]Hospital of Dermatology, Chinese Academy of Medical Sciences and Peking Union Medical College, Nanjing, [2]Beijing Deeperception Technology Ltd, Beijing and 3The First Affiliated Hospital of Nanjing Medical University, Nanjing, China

Since the results of basic and specific classification in male androgenetic alopecia are subjective, and trichoscopic data, such as hair density and diameter distribution, are potential quantitative indicators, the aim of this study was to develop a deep learning framework for automatic trichoscopic image analysis and a quantitative model for predicting basic and specific classification in male androgenetic alopecia. A total of 2,910 trichoscopic images were collected and a deep learning framework was created on convolutional neural networks. Based on the trichoscopic data provided by the framework, correlations with basic and specific classification were analysed and a quantitative model was developed for predicting basic and specific classification using multiple ordinal logistic regression. A deep learning framework that can accurately analyse hair density and diameter distribution on trichoscopic images and a quantitative model for predicting basic and specific classification in male androgenetic alopecia were established.

Key words: deep learning; androgenetic alopecia; trichoscopic image; BASP classification.

Accepted Dec 22, 2021; Epub ahead of print Dec 22, 2021

Acta Derm Venereol 2022; 102: adv00635.

Corr: Yiqun Jiang, and Wei Hou, Hospital of Dermatology, Chinese Academy of Medical Sciences and Peking Union Medical College, #12 Jiangwangmiao Road, Nanjing, Jiangsu, China. E-mail: yiqunjiang@qq.com; houwei210042@139.com

SIGNIFICANCE

Androgenetic alopecia is the most common form of hair loss and basic and specific classification is a regular grading standard for it. However, the classification mainly depends on clinicians' subjective judgment and often comes with inconsistent results. To solve this problem, we developed an artificial intelligence system to measure hair density and hair diameter in the trichoscopic images automatically. Then, these trichoscopic data were analyzed and a quantitative model for predicting basic and specific classification was created. This study provides an accurate tool for androgenetic alopecia grading, which is beneficial to the evaluation of therapeutic effects and follow-up of patients.

Androgenetic alopecia (AGA), the most common form of hair loss, usually manifests as typical male-pattern baldness in men and is related to heredity, androgen level and its receptors (1). The pathophysiological feature of AGA is hair follicular miniaturization. Early diagnosis and accurate assessment of severity play an important role in the treatment and follow-up of AGA (2).

Male AGA is characterized by progressive hair thinning in the temporal, frontal and vertex areas (3). In clinical practice, basic and specific (BASP) classification is a commonly used grading standard for male AGA, which demonstrates the varying degrees of pattern hair loss. The basic types represent the shape of the hairline, and the specific types represent the degree of hair sparsity in the frontal and vertex areas (4). However, the classification of specific types depends mainly on clinicians' subjective judgement. Lack of quantitative indicators may lead to inconsistent results among different practitioners and different visits, resulting in evaluation confusion. Some studies have found that hair density and the percentage of vellus hairs change with the progression of hair loss, but the relevance is inconclusive (5, 6).

Due to the convenience and non-invasiveness of trichoscopy, this technique is used clinically to measure hair density and hair diameters. However, the currently available software for trichoscopic image analysis generates inaccurate results compared with visual counting (7, 8). An accurate method of analysis is needed for trichoscopic imaging. Recently, deep learning frameworks have developed rapidly in medical image recognition. Through training with a large dataset, automatic image recognition models with high accuracy can be established (9, 10). We have previously developed a deep learning framework for detecting smartphone-captured microscopic images (11).

The aim of the current study was to develop a deep learning framework for automatic trichoscopic image analysis to accurately measure hair density and hair diameter distribution. The trichoscopic characteristics of male AGA were then evaluated, based on the established framework, and a quantitative model for predicting BASP classification was developed.

doi: 10.2340/actadv.v101.564

MATERIALS AND METHODS

Study population and image acquisition

The study subjects included outpatients who attended the Hospital of Dermatology, Chinese Academy of Medical Sciences and Peking Union Medical College from January 2019 to June 2019. Diagnoses of AGA or normal subject were made, and AGA was graded according to the BASP classification by consensus among 3 independent dermatologists (YJ, WH and JN, with >5 years of experience evaluating hair disorders). Patients with other hair loss diseases, such as diffuse alopecia areata and telogen effluvium, or scalp disorders, were excluded.

Because most patients refused to shave their hair, trichoscopic images were captured without patients having their hair cut. In all patients the hair was combed to the side along the midline. DermDOC® dermoscopy (Derma Medical Systems Inc., Vienna, Austria) was used to obtain trichoscopic images at the frontal, vertex, temporal and occipital areas for every subject. The measurement point of the frontal, vertex and occipital areas were located roughly 12, 24 and 30 cm above the middle of the glabella, respectively. Temporal images were taken at 6 cm from the external ear canals. Image acquisition was performed with 30× magnification. A total of 2,910 trichoscopic images were collected. All participants signed a written informed consent and the study protocol was reviewed and approved by the Institutional Review Board of the Hospital of Dermatology, Chinese Academy of Medical Sciences and Peking Union Medical College.

Manual annotation of trichoscopic images

A manual annotation tool was written in C++ to mark hairs and to measure the diameters of hair shafts in the trichoscopic images. Researchers annotated each hair with 2 points from the hair follicle opening to the proximal part of the hair shaft. The diameter of hair shaft was then measured and 3 colours were used to label 3 types of hairs (blue for vellus hairs <0.03 mm diameter; green for intermediate hairs 0.03–0.06 mm diameter, and red for terminal hairs >0.06 mm diameter). The annotated trichoscopic images are shown in Fig. S1. After annotation, 2,910 images were included in the dataset and randomly divided into 3 sets, of which 2,310 images were used for training, 300 for validation and 300 for testing. The images in each set were from different participants and had no overlay.

Deep learning framework for automatic trichoscopic image analysis

To accurately predict the hair density and hair diameter distribution on trichoscopic images, a deep learning framework for automatic trichoscopic image analysis was proposed. This model contained 2 types of convolutional neural networks (CNN): the detection net (D-Net) structure for detecting hair follicle openings and the regression net (R-Net) structure for predicting the number of hairs and the proportion of vellus hairs, intermediate hairs and terminal hairs (**Fig. 1**).

D-Net. D-Net is a type of fully convolutional network (FCN), which has mostly been applied to solve cascading target detection and image segmentation tasks (12). This structure applies convolution instead of sliding window, which allows images input at any size (Fig. S2). Trichoscopic images were input to the D-Net at a size of 1280*720*3. Then the size was doubled to 2560*1440*3 and an 80*80 sliding window was used to extract the images. The D-Net had 6 Residual Net units to process the data. Finally, the model got 2 vectors with 1*1*2 and 1*1*4 through FCN layer. It applied the softmax function to predict whether the images contained hair follicle openings and the 4 points of the bounding box (13).

R-Net. Based on the detected locations of hair follicle openings, a multi-task R-Net was applied to predict the number of hairs and the proportion of vellus hairs, intermediate hairs and terminal hairs. The R-Net was based on MobileNet, which is a convolutional network mostly used for mobile and embedded vision applications (14). Different from the MobileNet, the R-Net had another fully-connected layer for predicting the proportions of 3 types of hairs after the average pooling layer.

Experimental settings. Before training, the Hue, Saturation, Value colour model was applied (15) to deal with different skin tones. The model was implemented on the NVIDIA Titan Xp (NVIDIA Inc., California, USA). This graphics processing unit was driven by 3,840 NVIDIA CUDA cores running at 1.6 GHz and packed 12 TFLOPS of brute force.

For D-Net, the maximum training iteration was 60. Each iteration contained 49 batch sizes, and each batch had 64 images. The initial learning rate of the model was 0.0025, and the Nesterov Accelerated Gradient (16) was adopted to optimize the objective. The maximum training iteration of R-Net was 30. Each iteration had 785 batch sizes, and each batch contained 64 samples. The initial learning rate of R-Net was 0.001, and was reduced by half every 10 batches. The Stochastic Gradient Descent method (17) was applied to optimize the objective of R-Net, where the weight decay was 0.0005 and the momentum was set to 0.9.

Performance evaluation

This paper adopted mean accuracy method for evaluating the D-Net.

$$precision = \frac{tp}{tp + fp} = \frac{tp}{n}$$

where tp denotes the number of true predicted samples, fp represents the number of false predicted samples, and n is the total number of testing samples.

For R-Net, mean absolute error (MAE) (18) was applied, which can better reflect the actual situation of predicted value. The computational formula was introduced as below:

$$\mathrm{MAE(x)} = \frac{1}{m}\sum_{i=1}^{m}\left|y'^{(i)} - y^{(i)}\right|$$

where, y' represents the true value, y denotes the predicted value, and m is the number of samples.

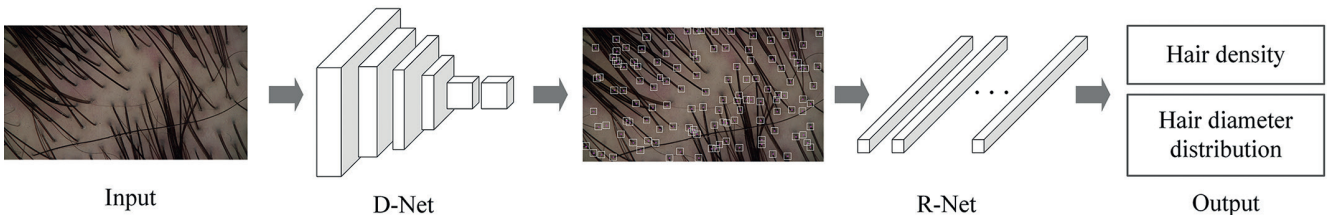

Fig. 1. Structure of automatic trichoscopic image analysis model. There were 2 stages: D-Net for detection and R-Net for prediction. When inputting a trichoscopic image to the D-Net, the bounding boxes of hair follicle openings were detected. Then, based on the detected area, the R-Net predicted the number of hairs and the proportion of vellus hairs, intermediate hairs and terminal hairs.

Collection of clinical and trichoscopic data

Patients' age, BASP grading and trichoscopic data in the frontal and vertex areas were collected. Trichoscopic data included hair density (total number of hairs per 1 cm^2 area) and hair diameter distribution (percentage of vellus hairs, intermediate hairs and terminal hairs out of the total number of hairs).

Statistical analysis

Descriptive statistics for continuous variables were reported as means ± standard deviations (SD). Group comparisons were performed using unpaired Student's *t*-test or analysis of variance (ANOVA). Multiple ordinal logistic regression was conducted to explore the association of ordinal categorical outcomes with multiple exposures. The fitness of the model was evaluated by cross-validation. SPSS software 26.0 (SPSS Inc., Chicago, IL, USA) was used for analysis. All statistical tests and confidence intervals were 2-sided with a significance level of 0.05.

RESULTS

Performance evaluation of the deep learning framework

The results of performance evaluation for D-Net and R-Net are shown in **Table I**. Intuitively, during the period of hair detection, D-Net achieved an accuracy of 95.44%. The R-Net was tested based on 2 kinds of data, 1 was manually-labelled hair follicle regions (noted as R-Net1), and the other was the predicted hair follicle regions of D-Net (noted as R-Net2).

During testing, a trichoscopic image was input and the number of hairs output. It took 2 s for testing the whole model, where 135 ms for detection and approximately 20 ms for prediction. Four samples were randomly selected from the D-Net and R-Net (the results are shown in **Fig. 2**).

Table I. Results of performance evaluation for D-Net and R-Net

Model	Precision %	MAE in predicting the total number of hairs	MAE in predicting the proportion of 3 types of hairs		
			Terminal hairs (%)	Intermediate hairs (%)	Vellus hairs (%)
D-Net	95.44	–	–	–	–
R-Net1	–	11.03	6.81	8.40	6.56
R-Net2	–	25.05	8.76	8.27	9.30

The precision of D-Net was evaluated using mean accuracy method. Mean absolute error (MAE) was applied to assess the performance of R-Net in predicting total number of hairs and the proportion of 3 types of hairs. The R-Net was tested based on 2 kinds of data, 1 was manually-labelled hair follicle regions (noted as R-Net1), and the other was the predicted hair follicle regions of D-Net (noted as R-Net2).

Changes in hair parameters with the progression of baldness

A total of 582 subjects were enrolled in the study. The normal group included 54 subjects aged 18–53 years (mean ± SD age 29.87 ± 8.79 years). The AGA group comprised 528 subjects aged 18–55 years (mean ± SD age 29.30 ± 7.60 years). All participants were divided into 4 groups according to the BASP grading and grade 0 group included normal subjects and patients without baldness in the frontal or vertex area. The results for hair density and hair thickness analysis are shown in **Table II** and **Fig. 3**. In both frontal and vertex areas, the percentage of vellus hairs, intermediate hairs and terminal hairs were significantly different among 4 groups, while hair density was similar. Further pairwise comparisons were made and the results revealed that the percentage of vellus hairs and terminal hairs were significantly different between either 2 groups. The percentage of intermediate hairs was statistically similar between patients with grade 2 and grade 3 baldness, while the differences between the remaining groups were significant. With an increase in BASP grade, the percentage of

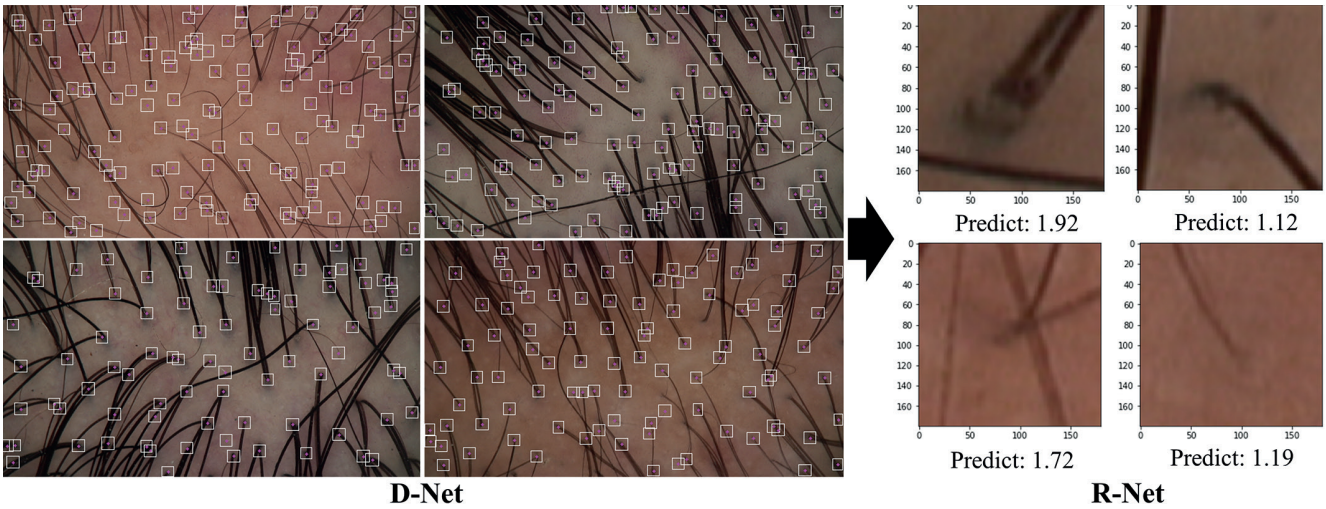

Fig. 2. Detected samples of D-Net and predicted samples of R-Net. Four detected samples of D-Net are shown in the left. Hair follicle openings were detected in the bounding boxes. Apparently, the D-Net model achieved a high performance in detecting the location of hair follicle openings. The right panel shows 4 predicted samples of R-Net. The rounded number of hairs in each sample was 2, 1, 2 and 1, respectively, which were the same as the real values, demonstrating the high prediction accuracy of the R-Net model.

Table II. Hair density and percentage of vellus hairs, intermediate hairs and terminal hairs of the subjects

Classification	0	1	2	3
Frontal, *n*	67	289	193	33
Hair density, hairs cm^{-2}, mean±SD	244±35	247±37	247±42	247±59
Vellus hairs, %, mean±SD	9±2	17±4	28±6	47±4
Intermediate hairs, %, mean±SD	23±3	34±6	41±7	41±4
Terminal hairs, %, mean±SD	68±4	49±7	31±8	13±3
Vertex, n	67	252	217	46
Hair density, hairs cm^{-2}, mean±SD	243±37	248±45	247±43	254±56
Vellus hairs, %, mean±SD	9±3	17±5	27±5	48±4
Intermediate hairs, %, mean±SD	23±3	32±6	43±6	41±3
Terminal hairs, %, mean±SD	69±5	51±9	30±8	10±3

The participants were divided into 4 groups according to the BASP grading and grade 0 group included normal control and patients without baldness in the frontal or vertex area. Trichoscopic data including hair density (the total number of hairs per 1 cm^2 area) and hair diameter distribution (the percentage of vellus hairs, intermediate hairs and terminal hairs out of the total number of hairs) in the frontal and vertex areas were collected.

vellus hairs and intermediate hairs showed an increasing trend while the percentage of terminal hairs showed a declining trend.

A quantitative model for predicting basic and specific classification in male androgenic alopecia

In both frontal and vertex areas, 90% of the samples were used as a training set and 10% were used as a testing set. The percentage of vellus hairs and intermediate hairs were selected as independent variables, and multiple ordinal logistic regression was conducted. In the frontal area, the fitting equations were expressed as follows:

Ln(odds, P≤0)=14.905–0.634×vellus hairs(%)–0.307×intermediate hairs(%)

Ln(odds, P≤1)=25.822–0.634×vellus hairs(%)–0.307×intermediate hairs(%)

Ln(odds, P≤2)=39.262–0.634×vellus hairs(%)–0.307×intermediate hairs(%)

In the vertex area, the fitting equations were expressed as follows:

Ln(odds, P≤0)=13.226–0.543×vellus hairs(%)–0.305×intermediate hairs(%)

Ln(odds, P≤1)=23.350–0.543×vellus hairs(%)–0.305×intermediate hairs(%)

Ln(odds, P≤2)=35.401–0.543×vellus hairs(%)–0.305×intermediate hairs(%)

(odd=P/(1–P), P represents cumulative probability)

Finally, the probability of each grade was calculated according to the following formula:

$$P0=\frac{e^{ln\,(odds,P\le 0)}}{1+e^{ln\,(odds,P\le 0)}}$$

$$P1=\frac{e^{\ln\,(odds,P\le 1)}}{1+e^{\ln\,(odds,P\le 1)}}-\frac{e^{\ln\,(odds,P\le 0)}}{1+e^{\ln\,(odds,P\le 0)}}$$

$$P2=\frac{e^{\ln\,(odds,P\le 2)}}{1+e^{\ln\,(odds,P\le 2)}}-\frac{e^{\ln\,(odds,P\le 1)}}{1+e^{\ln\,(odds,P\le 1)}}$$

P3=1-(P0+P1+P2)

According to these equations, the probability of each grade of BASP classification in the testing set was calculated and the grade with the highest probability was the predicted grade. Then cross-validation was performed to analyse the accuracy of this predictive model. In the frontal and vertex area, the number of samples that the

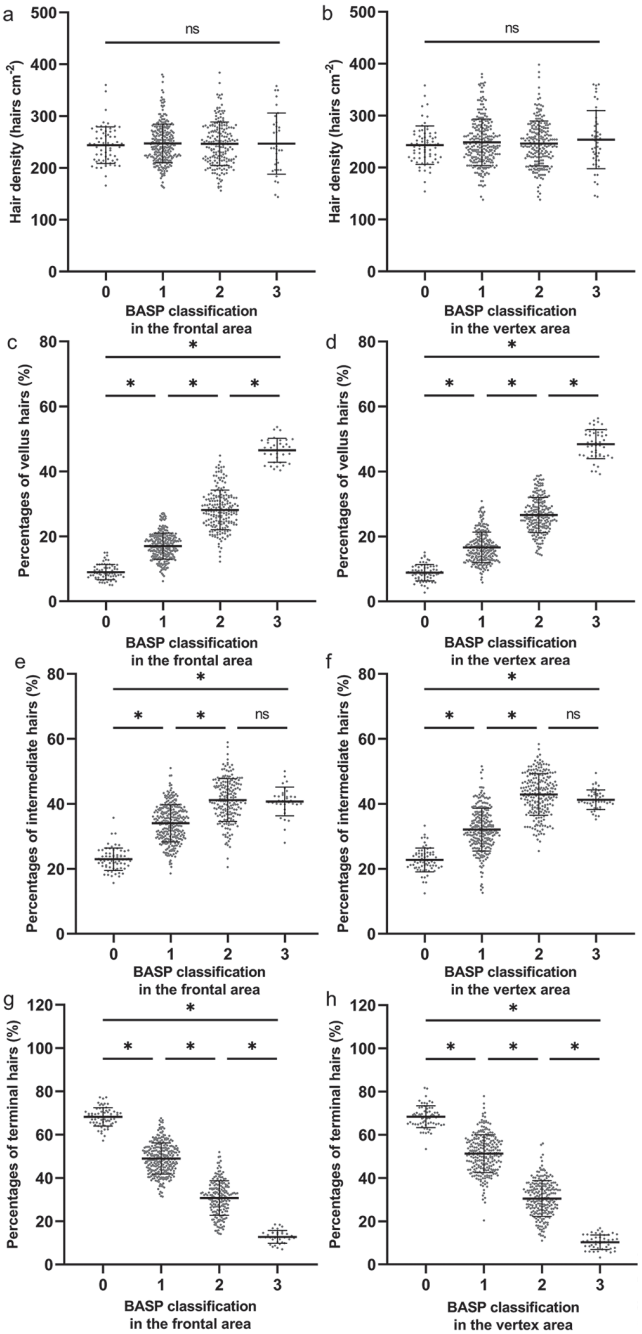

Fig. 3. Distribution of hair density and hair thickness in study subjects. The participants were divided into 4 groups according to the BASP grading and grade 0 group included normal subjects and AGA patients without baldness in the frontal or vertex area. (a, b) In both frontal and vertex areas, there is no significant difference in hair density among different groups. (c–h) In both frontal and vertex areas, the percentage of vellus hairs, intermediate hairs and terminal hairs were significantly different among 4 groups. With the rise of BASP grading, the percentage of vellus hairs showed an increasing trend, while the percentage of terminal hairs showed a decreasing trend. The percentage of intermediate hairs increased gradually from grade 0 to grade 2, but presented no significant difference between grade 2 and grade 3 (*$p < 0.001$).

model predicted correctly was 56 and 54, with an accuracy of 93% and 90%, respectively.

DISCUSSION

Artificial intelligence (AI) has been developed in recent decades to assist medical image recognition (19). Recently, deep learning, the state-of-the-art approach in the field of AI, has shown promising performances in computer vision tasks. Deep neural networks are composed of multiple layers, whereby higher level features can be extracted from lower level features. Unlike conventional machine learning techniques , which require human experts to design task-related features, deep neural networks extract features in a self-taught manner, which only requires training data with minor pre-processing when necessary (20). This distinct characteristic has laid the foundation for its unprecedented success in medical image recognition. Some studies have applied deep learning to hair loss evaluation, but there is currently no accurate framework to predict hair density and hair diameter distribution on trichoscopic images (21, 22).

This framework is a multi-task structure, containing 2 kinds of CNN: D-Net and R-Net. The D-Net was trained to detect hair follicle openings, while the R-Net was applied to predict hair density and hair diameter. Since most participants were reluctant to shave their hair, trichoscopic images were acquired without cutting their hair. Consequently, the hairs in the images crossed each other, making it difficult to distinguish each hair and measure the diameter of the hair shaft. To solve this problem, the hair follicle opening was chosen as the unique mark of each hair, and hair diameter was measured near the opening. After training, the performance of this framework was evaluated in the testing dataset, and the results of D-Net achieved an accuracy of 95.44%, comparable with other multi-label detection task (23). The MAE results of hair counts based on traditional method was approximately 40%, which was higher than the results of both R-Net1 and R-Net2 models, indicating the superior performance of R-Net (7). The experimental results revealed that this framework can achieve similar accuracy to manual labelling. Clinical application of this framework may liberate clinicians from mechanical image analysis and improve the efficiency of diagnosis.

Furthermore, this study analysed the trichoscopic characteristics of the subjects, including the hair density and the percentage of vellus hairs, intermediate hairs and terminal hairs, using the deep learning framework. Although the Hamilton-Norwood classification is used more widely in male AGA grading, it still has some limits. For example, patients of the same grade show different hair sparsity degrees in the frontal and vertex regions. Therefore, BASP classification was chosen to grade separate regions more accurately. All participants were divided into 4 groups according to BASP classification. In both frontal and vertex areas, the hair density presented wide variations between individuals. There was no significant difference in hair density among the 4 groups, which indicated that the contribution of hair density to global appearance was trivial. Previous studies have compared hair density in individuals with or without AGA, and the results were inconsistent. Rushton et al. compared the hair density in 26 subjects with male AGA and 13 normal controls, using a trichogram method, and found significant mean difference in the frontal-vertex area (24). However, this study had a relatively small sample that may affect the accuracy of the results. Whiting et al. analysed the scalp biopsy specimens of 106 male patients with AGA and 22 normal control subjects in the vertex region, and the result showed lower hair density for the AGA group, but the difference was not significant (25). Moreover, Ishino et al. (5) measured the hair density in 254 patients with male AGA and 115 normal controls using a videomicroscopy technique and no statistical difference was found, which was in accordance with the current results. The percentage of vellus hairs showed an increasing tendency, while the percentage of terminal hairs revealed a downward trend with the progression of baldness in all BASP types, which was consistent with the pathogenesis of AGA. The percentage of intermediate hairs increased from grade 0 to grade 2 baldness and was statistically similar between patients with grade 2 and grade 3 baldness. The fact that changes in intermediate hairs were more obvious in the early stages of hair loss was in coherence with the process of gradual miniaturization of hair follicles in AGA. The data above indicate that the percentage of vellus hairs, intermediate hairs and terminal hairs can be selected as quantitative grading indicators for male AGA.

Then we chose the percentage of vellus hairs and the percentage of intermediate hairs as independent variables and performed multiple ordinal logistic regression to establish a quantitative model for predicting BASP classification in male AGA. The cross-validation showed that the accuracy of this model was approximately 90%. This work opens a new avenue for quantitative BASP classification in different clinical scenarios. However, some limitations still exist. The sample size of this study is small and most of the participants are Chinese. Considering hairs of different races vary in colour and density, the quantitative model for predicting BASP classification may be more applicable to Asian populations. More data from different regions are necessary to improve the model.

In conclusion, this study proposed a deep learning framework that can analyse trichoscopic images without hair shaving, providing accurate information about hair density and diameter distribution. It was found that the percentage of vellus hairs, the percentage of intermediate hairs, and the percentage of terminal hairs were closely related to the severity of hair loss, and can be used as

quantitative grading indicators for male AGA. Finally, a quantitative model for predicting BASP classification in male AGA was established. This is a useful tool for predicting BASP classification in a highly reproducible, easily applicable, and quantifiable manner.

ACKNOWLEDGEMENTS

This study was supported by CAMS Innovation Fund for Medical Sciences (2021-I2M-C&T-B-087), CAMS Innovation Fund for Medical Sciences (CIFMS-2017-I2M-1-017) and the Nanjing Incubation Program for National Clinical Research Center (2019060001).

The authors have no conflicts of interest to declare.

REFERENCES

1. Lolli F, Pallotti F, Rossi A, Fortuna MC, Caro G, Lenzi A, et al. Androgenetic alopecia: a review. Endocrine 2017; 57: 9–17.
2. Ellis JA, Sinclair R, Harrap SB. Androgenetic alopecia: pathogenesis and potential for therapy. Expert Rev Mol Med 2002; 4: 1–11.
3. Hamilton JB. Patterned loss of hair in man; types and incidence. Ann N Y Acad Sci 1951; 53: 708–728.
4. Lee WS, Ro BI, Hong SP, Bak H, Sim WY, Kim DW, et al. A new classification of pattern hair loss that is universal for men and women: basic and specific (BASP) classification. J Am Acad Dermatol 2007; 57: 37–46.
5. Ishino A, Takahashi T, Suzuki J, Nakazawa Y, Iwabuchi T, Tajima M. Contribution of hair density and hair diameter to the appearance and progression of androgenetic alopecia in Japanese men. Br J Dermatol 2014; 171: 1052–1059.
6. Hayashi S, Miyamoto I, Takeda K. Measurement of human hair growth by optical microscopy and image analysis. Br J Dermatol 1991; 125: 123–129.
7. Van Neste D, Trüeb RM. Critical study of hair growth analysis with computer-assisted methods. J Eur Acad Dermatol Venereol 2006; 20: 578–583.
8. Saraogi PP, Dhurat RS. Automated digital image analysis (TrichoScan®) for human hair growth analysis: ease versus errors. Int J Trichology 2010; 2: 5–13.
9. Du-Harpur X, Watt FM. What is AI? Applications of artificial intelligence to dermatology. Br J Dermatol 2020; 183: 423–430.
10. Cullell-Dalmau M, Otero-Vinas M, Manzo C. Research techniques made simple: deep learning for the classification of dermatological images. J Invest Dermatol 2020; 140: 507–514.e501.
11. Jiang YQ, Xiong JH, Li HY, Yang XH, Yu WT, Gao M, et al. Recognizing basal cell carcinoma on smartphone-captured digital histopathology images with a deep neural network. Br J Dermatol 2020; 182: 754–762.
12. Shelhamer E, Long J, Darrell T. Fully convolutional networks for semantic segmentation. IEEE Trans Pattern Anal Mach Intell 2017; 39: 640–651.
13. Yan LC, Yoshua B, Geoffrey H. Deep learning. Nature 2015; 521: 436–444.
14. Howard AG, Zhu M, Chen B, Kalenichenko D, Wang W, Weyand T, et al. MobileNets: Efficient Convolutional Neural Networks for Mobile Vision Applications. [accessed 10th June 2019]. Available from: https://arxiv.org/abs/1704.04861.
15. Schwarz MW, Cowan WB, Beatty JC. An experimental comparison of RGB, YIQ, LAB, HSV, and opponent color models. ACM Transactions on Graphics (TOG) 1987; 6: 123–158.
16. Botev A, Lever G, Barber D. Nesterov's accelerated gradient and momentum as approximations to regularised update descent. 2017 International Joint Conference on Neural Networks (IJCNN): IEEE, 2017: p. 1899–1903.
17. Bottou L. Large-scale machine learning with stochastic gradient descent. In: Lechevallier Y, Saporta G, editors. Proceedings of COMPSTAT'2010. Heidelberg: Physica-Verlag HD; 2010: p. 177–186.
18. Willmott CJ, Matsuura K. Advantages of the mean absolute error (MAE) over the root mean square error (RMSE) in assessing average model performance. Climate Res 2005; 30: 79–82.
19. Yu KH, Beam AL, Kohane IS. Artificial intelligence in healthcare. Nat Biomed Eng 2018; 2: 719–731.
20. Shen D, Wu G, Suk HI. Deep Learning in medical image analysis. Annu Rev Biomed Eng 2017; 19: 221–248.
21. Urban G, Feil N, Csuka E, Hashemi K, Ekelem C, Choi F, et al. Combining deep learning with optical coherence tomography imaging to determine scalp hair and follicle counts. Lasers Surg Med 2021; 53: 171–178.
22. Lee S, Lee JW, Choe SJ, Yang S, Koh SB, Ahn YS, et al. Clinically applicable deep learning framework for measurement of the extent of hair loss in patients with alopecia areata. JAMA Dermatol 2020; 156: 1018–1020.
23. Liu W, Anguelov D, Erhan D, Szegedy C, Reed S, Fu C-Y, et al. Ssd: Single shot multibox detector. European conference on computer vision: Springer, 2016: p. 21–37.
24. Rushton DH, Ramsay ID, Norris MJ, Gilkes JJ. Natural progression of male pattern baldness in young men. Clin Exp Dermatol 1991; 16: 188–192.
25. Whiting DA. Diagnostic and predictive value of horizontal sections of scalp biopsy specimens in male pattern androgenetic alopecia. J Am Acad Dermatol 1993; 28: 755–763.